

# The Large Magellanic Cloud: Structure and Kinematics

By **Roeland P. van der Marel**

Space Telescope Science Institute, 3700 San Martin Drive, Baltimore, MD 21218

I review our understanding of the structure and kinematics of the Large Magellanic Cloud (LMC), with a particular focus on recent results. This is an important topic, given the status of the LMC as a benchmark for studies of microlensing, tidal interactions, stellar populations, and the extragalactic distance scale. I address the observed morphology and kinematics of the LMC; the angles under which we view the LMC disk; its in-plane and vertical structure; the LMC self-lensing contribution to the total microlensing optical depth; the LMC orbit around the Milky Way; and the origin and interpretation of the Magellanic Stream. Our understanding of these topics is evolving rapidly, in particular due to the many large photometric and kinematic datasets that have become available in the last few years. It has now been established that: the LMC is considerably elongated in its disk plane; the LMC disk is thicker than previously believed; the LMC disk may have warps and twists; the LMC may have a pressure-supported halo; the inner regions of the LMC show unexpected complexities in their vertical structure; and precession and nutation of the LMC disk plane contribute measurably to the observed line-of-sight velocity field. However, many open questions remain and more work is needed before we can expect to converge on a fully coherent structural, dynamical and evolutionary picture that explains all observed features of the LMC.

---

## 1. Introduction

The Large Magellanic Cloud (LMC) is one of our closest neighbor galaxies at a distance of  $\sim 50$  kpc. The Sagittarius dwarf is closer at  $\sim 24$  kpc, but its contrast with respect to the Milky Way foreground stars is so low that it was discovered only about a decade ago. The LMC is therefore the closest, big, easily observable galaxy from our vantage point in the Milky Way. As such, it has become a benchmark for studies on various topics. It is of fundamental importance for studies of stellar populations and the interstellar medium (ISM), it is being used to study the presence of dark objects in the Galactic Halo through microlensing (e.g., Alcock et al. 2000a), and it plays a key role in determinations of the cosmological distance scale (e.g., Freedman et al. 2001). For all these applications it is important to have an understanding of the structure and kinematics of the LMC. This is the topic of the present review. For information on other aspects of the LMC, the reader is referred to the book by Westerlund (1997). The book by van den Bergh (2000) discusses more generally how the properties of the LMC compare to those of other galaxies in the Local Group.

The Small Magellanic Cloud (SMC) at a distance of  $\sim 62$  kpc is a little further from us than the LMC, and is about 5 times less massive. Its structure is more irregular than that of the LMC, and it is less well studied and understood. Recent studies of SMC structure and kinematics include the work by Hatzidimitriou et al. (1997), Udalski et al. (1998), Stanimirovic et al. (1999, 2004), Kunkel, Demers & Irwin (2000), Cioni, Habing & Israel (2000b), Zaritsky et al. (2000, 2002), Crawl et al. (2001) and Maragoudaki et al. (2001). However, our overall understanding of SMC structure and kinematics has not evolved much since the reviews by Westerlund and van den Bergh. The present review is therefore restricted to the LMC.

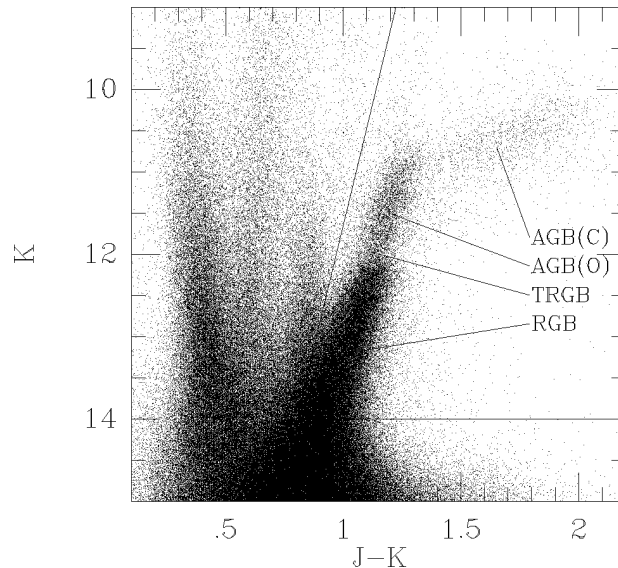


FIGURE 1. Near-IR ( $J - K_s, K_s$ ) CMD from 2MASS data for the LMC region of the sky. Only a quarter of the data is shown, to avoid saturation of the grey scale. The features due to the Red Giant Branch (RGB), the Tip of the RGB (TRGB), the oxygen-rich AGB stars [AGB(O)], and the carbon-rich AGB stars [AGB(C)] are indicated. The region enclosed by the solid lines was used to extract stars for creation of the LMC number density map in Figure 2.

## 2. Morphology

The LMC consists of an outer body that appears elliptical in projection on the sky, with a pronounced, off-center bar. The appearance in the optical wavelength regime is dominated by the bar, regions of strong star formation, and patchy dust absorption. The LMC is generally considered an irregular galaxy as a result of these characteristics. It is in fact the prototype of the class of galaxies called “Magellanic Irregulars” (de Vaucouleurs & Freeman 1973). Detailed studies of the morphological characteristics of the LMC have been performed using many different tracers, including optically detected starlight (Bothun & Thompson 1988; Schmidt-Kaler & Goehermann 1992), stellar clusters (Lynga & Westerlund 1963; Kontizas et al. 1990), planetary nebulae (Meatheringham et al. 1988) and non-thermal radio emission (Alvarez, Aparici & May 1987). Recent progress has come primarily from studies of stars on the Red Giant Branch (RGB) and Asymptotic Giant Branch (AGB) and from studies of HI gas.

### 2.1. Near-Infrared Morphology

Recently, two important near-IR surveys have become available for studies of the Magellanic Clouds, the Two Micron All Sky Survey (2MASS; e.g., Skrutskie 1998) and the Deep Near-Infrared Southern Sky Survey (DENIS; e.g., Epchtein et al. 1997). Cross-correlations of the data from these surveys and from other catalogs are now available as well (Delmotte et al. 2002). The surveys are perfect for a study of LMC morphology and structure. Near-IR data is quite insensitive to dust absorption, which is a major complicating factor in optical studies (Zaritsky, Harris & Thompson 1997; Zaritsky 1999; Udalski et al. 2000; Alcock et al. 2000b). The surveys have superb statistics with of the order of a million stars. Also, the observational strategy with three near-IR bands ( $J, H$  and  $K_s$  in the 2MASS survey;  $I, J$  and  $K_s$  in the DENIS survey) allows clear separation

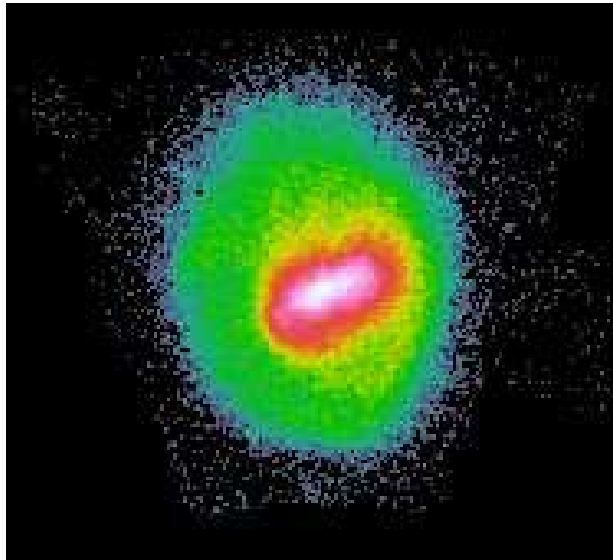


FIGURE 2. Surface number density distribution on the sky of RGB and AGB stars in the LMC from van der Marel (2001). North is to the top and east is to the left. The image covers an area of  $23.55^\circ \times 21.55^\circ$ . The Galactic foreground contribution was subtracted. A color version of the image is available at <http://www.stsci.edu/~marel/lmc.html> .

of different stellar populations. In particular, the data are ideal for studies of evolved RGB and AGB stars, which emit much of their light in the near-IR. This is important for studies of LMC structure, because these intermediate-age and old stars are more likely to trace the underlying mass distribution of the LMC disk than younger populations that dominate the light in optical images.

Figure 1 shows the  $(J - K_s, K_s)$  color-magnitude diagram (CMD) for the LMC region of the sky. Several finger-like features are visible, each due to different stellar populations in the LMC or in the foreground (Nikolaev & Weinberg 2000; Cioni et al. 2000a; Marigo, Girardi & Chiosi 2003). The LMC features of primary interest in the present context are indicated in the figure, namely the Red Giant Branch (RGB), the Tip of the RGB (TRGB), the oxygen-rich AGB stars, and the carbon-rich AGB stars (“carbon stars”). Van der Marel (2001) used the color cut shown in the figure to extract a sample from the 2MASS and DENIS datasets that is dominated by RGB and AGB stars. These stars were used to make the number-density map of the LMC shown in Figure 2. Kontizas et al. (2001) showed the distribution on the sky of  $\sim 7000$  carbon stars identified by eye from optical objective prism plates. Their map does not show all the rich detail visible in Figure 2, but it is otherwise in good agreement with it.

The near-IR map of the LMC is surprisingly smooth. The morphology is much less irregular than it is for the the younger stellar populations that dominate the optical light. Apart from the central bar there is a hint of some spiral structure, as discussed previously by, e.g., de Vaucouleurs & Freeman (1973). However, the spiral features all have very low contrast with respect to their surroundings, and there is certainly no well organized spiral pattern in the LMC. Quantitative analysis can be performed on the basis of ellipse fits to the number density contours. This yields a surface number density profile that can be fit reasonably well fit by an exponential with a scale length of  $1.4^\circ$  (1.3 kpc). The radial profiles of the ellipticity  $\epsilon$  (defined as  $1 - q$ , where  $q$  is the axial ratio) and the major axis

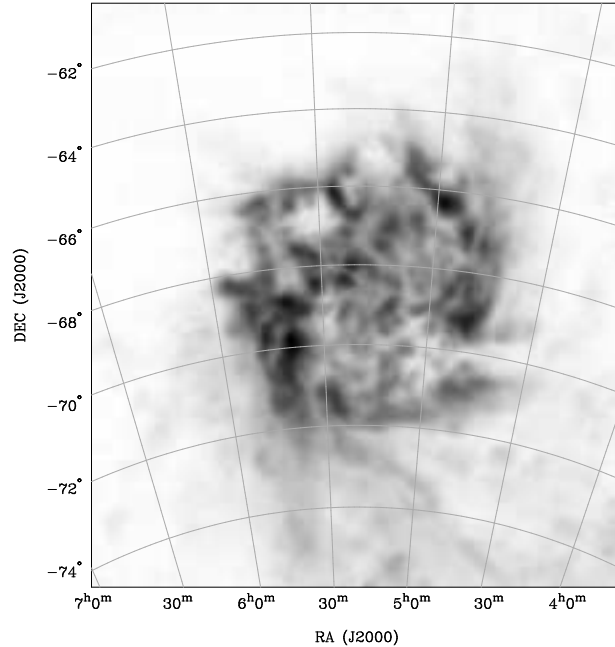


FIGURE 3. Peak brightness temperature image of HI in the LMC from Staveley-Smith et al. (2003). The data are from a Parkes multibeam survey and are sensitive to spatial structure in the range 200 pc to 10 kpc. The orientation is the same as in Figure 2, but the present image covers an area that is approximately 2.5 times smaller (i.e., 1.6 in each dimension).

position angle  $PA_{\text{maj}}$  both show pronounced variations as function of distance from the LMC center, due to the presence of the central bar. However, at radii  $r \gtrsim 4^\circ$  the contour shapes converge to an approximately constant position angle  $PA_{\text{maj}} = 189.3^\circ \pm 1.4^\circ$  and ellipticity  $\epsilon = 0.199 \pm 0.008$ .

## 2.2. HI Morphology

To study the distribution of HI in the LMC on small scales requires many pointings to cover the LMC at high angular resolution. Kim et al. (1998) used the Australia Telescope Compact Array (ATCA) to obtain a map that is sensitive on scales of 15–500 pc. On these scales, the morphology is dominated by HI filaments with numerous shells and holes. The turbulent and fractal nature of the ISM on these scales is the result of dynamical feedback into the ISM from star formation processes. In the context of the present review we are more interested in the large scale distribution of HI gas. This issue has been studied for decades, including work by McGee & Milton (1966), Rohlfs et al. (1984) and Luks & Rohlfs (1992). Most recently, Staveley-Smith et al. (2003) obtained the map shown in Figure 3, using a multibeam survey with the Parkes telescope. This map is sensitive to spatial structure in the range 200 pc to 10 kpc. The HI distribution is very patchy (see also Kim et al. 2003, who combined the data of Kim et al. [1998] and Staveley-Smith et al. [2003] into a single map that is sensitive to structures on all scales down to 15 pc). The HI in the LMC is not centrally concentrated and the brightest areas are several degrees from the center. The overall distribution is approximately circular and there is no sign of a bar. All of these characteristics are strikingly different from the stellar distribution shown in Figure 2.

Figure 4 shows contours of the HI distribution on a somewhat larger scale, from the

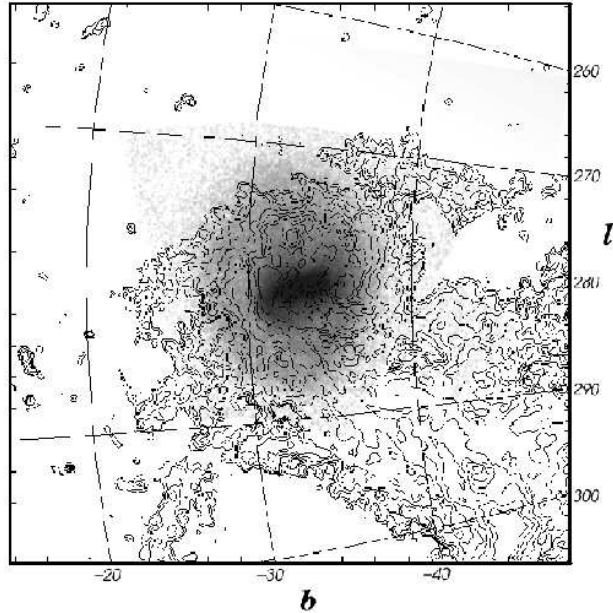


FIGURE 4. Contours of HI column density from Putman et al. (2003) overlaid on the LMC near-IR star count map from Figure 2. This figure is in Galactic coordinates, but  $(l, b)$  are shown so as to allow easy comparison with Figures 2 and 3. North is  $9^\circ$  clockwise from the vertical direction on the page. The image covers an area that is approximately 2.5 times larger than Figure 2 (i.e., 1.6 times in each dimension). The figure was kindly provided by M. Putman.

HIPASS data presented in Putman et al. (2003), overlaid on the LMC near-IR star count map from Figure 2. This comparison suggests that collisionless tracers such as RGB and AGB stars are best suited to study the structure and mass distribution of the LMC disk, whereas HI gas may be better suited to study the effects of tidal interactions. The stream of gas towards the right of Figure 4 is the start of the Magellanic Bridge towards the SMC, which provides one of the many pieces of evidence for strong tidal interactions between the LMC, the Milky Way and the SMC.

### 3. Magellanic Stream

Figure 5 shows a wide-area HI map of the Magallanic System. The most prominent feature is the Magellanic Stream, a  $10^\circ$  wide filament with  $\sim 2 \times 10^8 M_\odot$  of neutral hydrogen that spans more than  $100^\circ$  across the sky (e.g., Westerlund 1997; Putman et al. 2003). It consists of gas that trails the Magellanic Clouds as they orbit the Milky Way. A less prominent leading gas component was recently discovered as well (Lu et al. 1998; Putman et al. 1998), the start of which is seen at the left in Figure 5.

Many detailed theoretical models have been constructed for the Magellanic Stream (e.g., Murai & Fujimoto 1980; Lin & Lynden-Bell 1982; Shuter 1992; Liu 1992; Heller & Rohlfs 1994; Gardiner, Sawa & Fujimoto 1994; Moore & Davis 1994; Lin, Jones & Klemola 1995; Gardiner & Noguchi 1996; Yoshizawa & Noguchi 2003; Mastropietro et al. 2004; Connors et al. 2004). Models in which tidal stripping is the dominating process have been particularly successful. The most sophisticated recent calculations in this class are those by Yoshizawa & Noguchi (2003) and Connors et al. (2004), both of which build

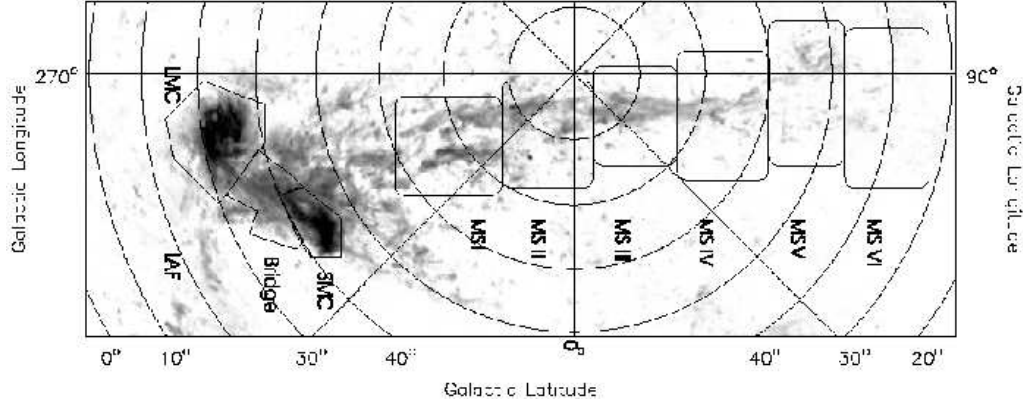


FIGURE 5. HI column density map of the Magellanic System in galactic coordinates from Putman et al. (2003). The LMC and SMC are indicated, as well as the Magellanic Bridge between them, several individual gas clumps in the Magellanic Stream (MS#), and the start of the Leading Arm Feature (LAF). The orientation of the LMC on the map is similar to that in Figure 4.

on earlier work by Gardiner & Noguchi (1996). In these models the LMC and SMC form a gravitationally bound system that orbits the Milky Way. The Magellanic Stream and the Leading Arm represent material that was stripped from the SMC  $\sim 1.5$  Gyr ago. This was the time of the previous perigalactic passage, which coincided with a close encounter between the Clouds. The models successfully reproduce many properties of the Magellanic Stream, including its position, morphology, width variation, and the velocity profile along the Stream. The models also explain the presence of the Leading Arm, and why it is less prominent than the trailing Stream.

Given the successes of tidal models, it has always been surprising that no population of stars associated with the Stream has ever been found (e.g., Irwin 1991; Guhathakurta & Reitzel 1998; Majewski et al. 2003). In a tidal model where the stripping is dominated by gravity, one might naively expect that both stars and gas are stripped equally. However, galaxies generally have HI gas disks that are more extended than the stellar distribution. Since material is preferentially stripped from the outskirts of a galaxy, this can explain why there may not be any stars associated with the Stream (Yoshizawa & Noguchi 2003). Alternatively, it has been argued that the lack of stars in the Stream may point to important contributions from other physical processes than tidal effects. For example, Moore & Davis (1994) and Mastropietro et al. (2004) suggest that the Stream consists of material which was ram-pressure stripped from the LMC during its last passage through a hot ( $\sim 10^6$  K) ionized halo component of the Milky Way. Another alternative was proposed by Heller & Rohlfs (1994), who suggested that hydrodynamical forces (rather than gravitational/tidal forces) during a recent LMC-SMC interaction are responsible for the existence of the Stream.

Models of the Magellanic Stream have traditionally used the properties of the Stream to estimate the orbit of the LMC, rather than to base the calculations on estimates of the LMC proper motion. An important characteristic of the orbit is the present-day tangential velocity in Galactocentric coordinates, for which values have been inferred that include  $v_{\text{LMC,tan}} = 369 \text{ km s}^{-1}$  (Lin & Lynden-Bell 1982),  $355 \text{ km s}^{-1}$  (Shuter 1992),  $352 \text{ km s}^{-1}$  (Heller & Rohlfs 1994),  $339 \text{ km s}^{-1}$  (Murai & Fujimoto 1980),  $320 \text{ km s}^{-1}$  (Liu 1992) and  $285 \text{ km s}^{-1}$  (Gardiner et al. 1994; Gardiner & Noguchi 1996), respectively. Proper motion measurements have improved significantly over time, and it is now known

that  $v_{\text{LMC,tan}} = 281 \pm 41 \text{ km s}^{-1}$  (as discussed in detail in Section 4). This is consistent with the lower range of the values predicted by models for the Stream. The data are most consistent with the models of Gardiner & Noguchi (1996) and their follow-ups, which also provide some of the best fits to many other properties of the Magellanic Stream. The observational error on  $v_{\text{LMC,tan}}$  is almost small enough to start ruling out some of the other models. It is possible that future proper motion measurements may yield a much more accurate determination of the LMC orbit. Models of the Magellanic Stream then hold the promise of providing important constraints on the mass, shape, and radial density profile of the Milky Way’s dark halo (e.g., Lin et al. 1995).

#### 4. Orbit

To understand the tidal interactions in the Magellanic System it is important to know the orbit of the LMC around the Milky Way. This requires knowledge of all three of the velocity components of the LMC center of mass. The line-of-sight velocity can be accurately determined from the Doppler velocities of tracers (see Section 5). By contrast, determination of the velocity in the plane of the sky is much more difficult. For the LMC, proper motion determinations are available from the following sources: Kroupa et al. (1994), using stars from the PPM Catalogue; Jones, Klemola & Lin (1994), using photographic plates with a 14 year epoch span; Kroupa & Bastian (1997), using Hipparcos data; Drake et al. (2002), using data from the MACHO project; and Anguita, Loyola & Pedreros (2000) and Pedreros, Anguita & Maza (2002), using CCD frames with an 11 year epoch span. Some of the measurements pertain to fields in the outer parts in the LMC disk, and require corrections for the orientation and rotation of the LMC disk. The measurements are all more-or-less consistent with each other to within the error bars. The exception to this is the Anguita et al. result, which almost certainly suffers from an unidentified systematic error. When this latter result is ignored, the weighted average of the remaining measurements yields proper motions towards the West and North of (van der Marel et al. 2002)

$$\mu_W = -1.68 \pm 0.16 \text{ mas yr}^{-1}, \quad \mu_N = 0.34 \pm 0.16 \text{ mas yr}^{-1}. \quad (4.1)$$

Transformation of the proper motion to a space velocity in  $\text{km s}^{-1}$  requires knowledge of the LMC distance  $D_0$ . Many techniques have been used over the years to estimate the LMC distance, but unfortunately, there continue to be systematic differences between the results from different techniques that far exceed the formal errors. It is beyond the scope of the present review to address this topic in detail. Instead, the reader is referred to the recent reviews by, e.g., Westerlund (1997), Gibson et al. (2000), Freedman et al. (2001) and Alves (2004b). Freedman et al. adopt a distance modulus  $m - M = 18.50 \pm 0.10$  on the basis of a review of all published work. This corresponds to  $D_0 = 50.1 \pm 2.5 \text{ kpc}$ . At this distance, a proper motion of  $1 \text{ mas yr}^{-1}$  corresponds to  $238 \pm 12 \text{ km s}^{-1}$  and 1 degree on the sky corresponds to  $0.875 \pm 0.044 \text{ kpc}$ .

Combination of the distance and proper motion of the LMC yields velocities  $v_W = -399 \text{ km s}^{-1}$  and  $v_N = 80 \text{ km s}^{-1}$  towards the West and North, respectively, with errors of  $\sim 40 \text{ km s}^{-1}$  in each direction. This can be combined with the observed line-of-sight velocity,  $v_{\text{sys}} = 262.2 \pm 3.4 \text{ km s}^{-1}$  (see Section 5.2), to obtain the three-dimensional motion of the LMC with respect to the Milky Way. It is usual to adopt a Cartesian coordinate system  $(X, Y, Z)$ , with the origin at the Galactic Center, the  $Z$ -axis pointing towards the Galactic North Pole, the  $X$ -axis pointing in the direction from the sun to the Galactic Center, and the  $Y$ -axis pointing in the direction of the sun’s Galactic Rotation. The observed LMC velocities must be corrected for the reflex motion of the sun, which is

easily done with use of standard estimates for the position and velocity of the sun with respect to the Galactic center. The  $(X, Y, Z)$  position of the LMC is then found to be (van der Marel et al. 2002)

$$\vec{r}_{\text{LMC}} = (-0.78, -41.55, -26.95) \text{ kpc}, \quad (4.2)$$

and its three-dimensional space velocity is

$$\vec{v}_{\text{LMC}} = (-56 \pm 36, -219 \pm 23, 186 \pm 35) \text{ km s}^{-1}. \quad (4.3)$$

This corresponds to a distance of 49.53 kpc from the Galactic center, and a total velocity of  $293 \pm 39 \text{ km s}^{-1}$  in the Galactocentric rest frame. The motion has a radial component of  $84 \pm 7 \text{ km s}^{-1}$  pointing away from the Galactic center, and a tangential component of  $281 \pm 41 \text{ km s}^{-1}$ . The proper motion of the SMC is known only with errors of  $\sim 0.8 \text{ mas yr}^{-1}$  in each coordinate (Kroupa & Bastian 1997), which is five times less accurate than for the LMC. However, to within these errors the SMC is known to have a galactocentric velocity vector that agrees with that of the LMC.

The combination of a small but positive radial velocity and a tangential velocity that exceeds the circular velocity of the Milky Way halo implies that the LMC must be just past pericenter in its orbit. The calculation of an actual orbit requires knowledge of the three-dimensional shape and the radial profile of the gravitational potential of the Milky Way dark halo. Gardiner et al. (1994) and Gardiner & Noguchi (1996) calculated orbits in a spherical Milky Way halo potential with a rotation curve that stays flat at  $220 \text{ km s}^{-1}$  out to a galactocentric distance of at least 200 kpc. Such a potential is consistent with our present understanding of the Milky Way dark halo (Kochanek 1996; Wilkinson & Evans 1999; Ibata et al. 2001). The calculations properly take into account that the LMC and SMC orbit each other while their center of mass orbits the Milky Way. However, since the LMC is more massive than the SMC, its motion is not too different from that of the LMC-SMC center of mass. For an assumed present-day LMC velocity  $\vec{v}_{\text{LMC}}$  consistent with that given in equation (4.3) the apocenter to pericenter ratio is inferred to be  $\sim 2.5 : 1$ . The perigalactic distance is  $\sim 45 \text{ kpc}$  and the orbital period around the Milky Way is  $\sim 1.5 \text{ Gyr}$ .

## 5. Kinematics

The kinematical properties of the LMC provide important clues to its structure. Observations have therefore been obtained for many tracers. The kinematics of gas in the LMC have been studied primarily using HI (e.g., Rohlfs et al. 1984; Luks & Rohlfs 1992; Kim et al. 1998). Discrete LMC tracers which have been studied kinematically include star clusters (Freeman, Illingworth & Oemler 1983; Schommer et al. 1992), planetary nebulae (Meatheringham et al. 1988), HII regions and supergiants (Feitzinger, Schmidt-Kaler & Isserstedt 1977), and carbon stars (Kunkel et al. 1997b; Graff et al. 2000; Alves & Nelson 2000; van der Marel et al. 2002). A common result from all these studies is that the line-of-sight velocity dispersion of the tracers is generally at least a factor  $\sim 2$  smaller than their rotation velocity. This implies that the LMC is kinematically cold, and must therefore to lowest approximation be a disk system.

### 5.1. General Expressions

To understand the kinematics of an LMC tracer population it is necessary to have a general model for the line-of-sight velocity field that can be fit to the data. All studies thus far have been based on the assumption that the mean streaming (i.e., the rotation) in the disk plane can be approximated to be circular. However, even with this simplifying



assumption it is not straightforward to model the kinematics of the LMC, because it is so near to us. Its main body spans more than  $20^\circ$  on the sky and one therefore cannot make the usual approximation that “the sky is flat” over the area of the galaxy. Spherical trigonometry must be used, which yields the general expression (van der Marel et al. 2002):

$$\begin{aligned} v_{\text{los}}(\rho, \Phi) = & s V(R') f \sin i \cos(\Phi - \Theta) \\ & + v_{\text{sys}} \cos \rho \\ & + v_t \sin \rho \cos(\Phi - \Theta_t) \\ & + D_0 (di/dt) \sin \rho \sin(\Phi - \Theta), \end{aligned} \quad (5.1)$$

with

$$R' = D_0 \sin \rho / f, \quad f \equiv \frac{\cos i \cos \rho - \sin i \sin \rho \sin(\Phi - \Theta)}{[\cos^2 i \cos^2(\Phi - \Theta) + \sin^2(\Phi - \Theta)]^{1/2}}. \quad (5.2)$$

In this equation,  $v_{\text{los}}$  is the observed component of the velocity along the line of sight. The quantities  $(\rho, \Phi)$  identify the position on the sky:  $\rho$  is the angular distance from the center and  $\Phi$  is the position angle with respect to the center (measured from North over East). The kinematical center is at the center of mass (CM) of the galaxy. The quantities  $(v_{\text{sys}}, v_t, \Theta_t)$  describe the velocity of the CM in an inertial frame in which the sun is at rest:  $v_{\text{sys}}$  is the systemic velocity along the line of sight,  $v_t$  is the transverse velocity, and  $\Theta_t$  is the position angle of the transverse velocity on the sky. The angles  $(i, \Theta)$  describe the direction from which the plane of the galaxy is viewed:  $i$  is the inclination angle ( $i = 0$  for a face-on disk), and  $\Theta$  is the position angle of the line of nodes, as illustrated in Figure 6. The line-of-nodes is the intersection of the galaxy plane and the sky plane. The velocity  $V(R')$  is the rotation velocity at cylindrical radius  $R'$  in the disk plane.  $D_0$  is the distance to the CM, and  $f$  is a geometrical factor. The quantity  $s = \pm 1$  is the ‘spin sign’ that determines in which of the two possible directions the disk rotates.

The first term in equation (5.1) corresponds to the internal rotation of the LMC. The second term is the part of the line-of-sight velocity of the CM that is seen along the line of sight, and the third term is the part of the transverse velocity of the CM that is seen along the line of sight. For a galaxy that spans a small area on the sky (very small  $\rho$ ), the second term is simply  $v_{\text{sys}}$  and the third term is zero. However, the LMC does not have a small angular extent and the inclusion of the third term is particularly important. It corresponds to a solid-body rotation component. Given the LMC transverse velocity implied by equation (4.1), it rises to an amplitude of  $71 \text{ km s}^{-1}$  at  $\rho = 10^\circ$ , which significantly exceeds the amplitude of the intrinsic rotation contribution (first term of eq. [5.1]) at that radius. The fourth term in equation (5.1) describes the line-of-sight component due to changes in the inclination of the disk with time, as are expected due to precession and nutation of the LMC disk plane as it orbits the Milky Way (Weinberg 2000). This term also corresponds to a solid-body rotation component.

The general expression in equation (5.1) appears complicated, but it is possible to gain some intuitive insight by considering some special cases. Along the line of nodes one has that  $\sin(\Phi - \Theta) = 0$  and  $\cos(\Phi - \Theta) = \pm 1$ , so that

$$\hat{v}_{\text{los}}(\text{along}) = \pm [v_{tc} \sin \rho - V(D_0 \tan \rho) \sin i \cos \rho]. \quad (5.3)$$

Here it has been defined that  $\hat{v}_{\text{los}} \equiv v_{\text{los}} - v_{\text{sys}} \cos \rho \approx v_{\text{los}} - v_{\text{sys}}$ . The quantity  $v_{tc} \equiv v_t \cos(\Theta_t - \Theta)$  is the component of the transverse velocity vector in the plane of the sky that lies along the line of nodes; similarly,  $v_{ts} \equiv v_t \sin(\Theta_t - \Theta)$  is the component perpendicular to the line of nodes. Perpendicular to the line of nodes one has that  $\cos(\Phi -$

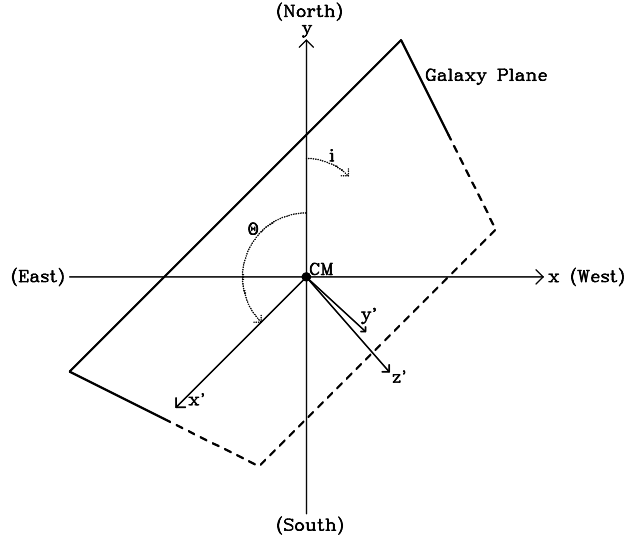


FIGURE 6. Schematic illustration of the observer’s view of the LMC disk. The plane of the disk is tilted diagonally out of the paper. The inclination  $i$  is the angle between the  $(x, y)$  plane of the sky, and the  $(x', y')$  plane of the galaxy disk. The  $x'$ -axis is the line of nodes, defined as the intersection of the  $(x, y)$  plane of the sky and the  $(x', y')$  plane of the galaxy disk. The angle  $\Theta$  is the position angle of the line of nodes in the plane of the sky.

$\Theta) = 0$  and  $\sin(\Phi - \Theta) = \pm 1$ , and therefore

$$\hat{v}_{\text{los}}(\text{perpendicular}) = \pm w_{ts} \sin \rho. \quad (5.4)$$

Here it has been defined that  $w_{ts} = v_{ts} + D_0(di/dt)$ . This implies that perpendicular to the line of nodes  $\hat{v}_{\text{los}}$  is linearly proportional to  $\sin \rho$ . By contrast, along the line of nodes this is true only if  $V(R')$  is a linear function of  $R'$ . This is not expected to be the case, because galaxies do not generally have solid-body rotation curves; disk galaxies tend to have flat rotation curves, at least outside the very center. This implies that, at least in principle, both the position angle  $\Theta$  of the line of nodes and the quantity  $w_{ts}$  are uniquely determined by the observed velocity field:  $\Theta$  is the angle along which the observed  $\hat{v}_{\text{los}}$  are best fit by a linear proportionality with  $\sin \rho$ , and  $w_{ts}$  is the proportionality constant.

### 5.2. Carbon Star Kinematics

Among the discrete tracers in the LMC that have been studied kinematically, carbon stars have yielded some of the largest and most useful datasets in recent years. Van der Marel et al. (2002) fitted the general velocity field expression in equation (5.1) to the data for 1041 carbon stars, obtained from the work of Kunkel et al. (1997a) and Hardy, Schommer & Suntzeff (unpublished). The combined dataset samples both the inner and the outer parts of the LMC, although with a discontinuous distribution in radius and position angle. Figure 7 shows the data, with the best model fit overplotted. Overall, the model provides a good fit to the data.

As discussed in Section 5.1, the line-of-nodes position angle is uniquely determined by the data; the model yields  $\Theta = 129.9^\circ \pm 6.0^\circ$ . The LMC inclination cannot be determined kinematically, but it is known reasonably well from other considerations (see Section 6). With both viewing angles and the LMC proper motion known, the rotation curve  $V(R')$  follows from equation (5.3). The result is shown in Figure 8. The inferred rotation curve

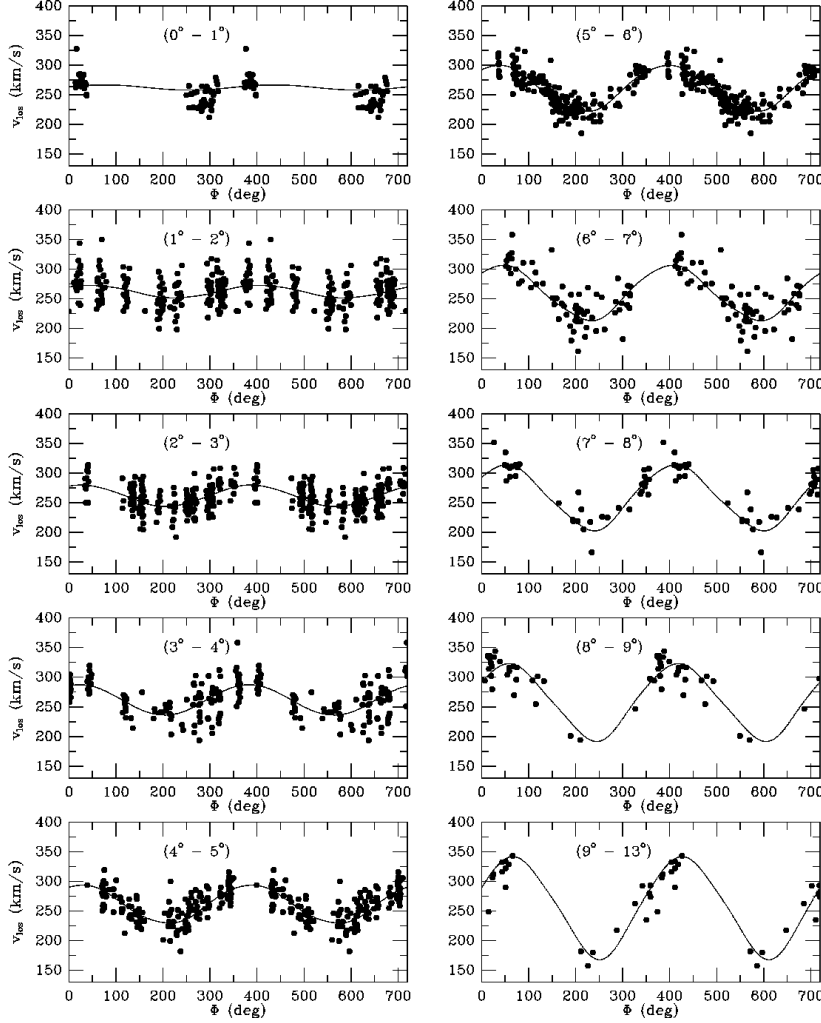


FIGURE 7. Carbon star line-of-sight velocity data from Kunkel, Irwin & Demers (1997a) and Hardy et al. (unpublished), as function of position angle  $\Phi$  on the sky. The displayed range of the angle  $\Phi$  is  $0^\circ$ – $720^\circ$ , so each star is plotted twice. Each panel corresponds to a different range of angular distances  $\rho$  from the LMC center, as indicated. The curves show the predictions of the best-fitting circularly-rotating disk model from van der Marel et al. (2002).

$V(R')$  rises linearly in the central region and is roughly flat at  $V \approx 50 \text{ km s}^{-1}$  for  $R' \gtrsim 4 \text{ kpc}$ . The negative value at the innermost radius  $R' \approx 0.5 \text{ kpc}$  has limited significance; it is probably affected by the sparse coverage of the data at these radii (see Figure 7), as well as potential non-circular streaming motions in the region of the bar. The error bars on  $V(R')$  in Figure 8 reflect the random errors due to the sampling of the data. However, there are also contributions from the errors in the line-of-nodes position angle  $\Theta$ , the LMC proper motion and the inclination  $i$ . In particular,  $V(R')$  scales as  $1/\sin i$ ; and if the component  $v_{tc}$  of the transverse velocity vector along the line of nodes is larger than given in equation (4.1), then  $V(R')$  will go up. When all uncertainties are properly accounted for, the amplitude of the flat part of the rotation curve and its formal error become  $V = 49.8 \pm 15.9 \text{ km s}^{-1}$ .

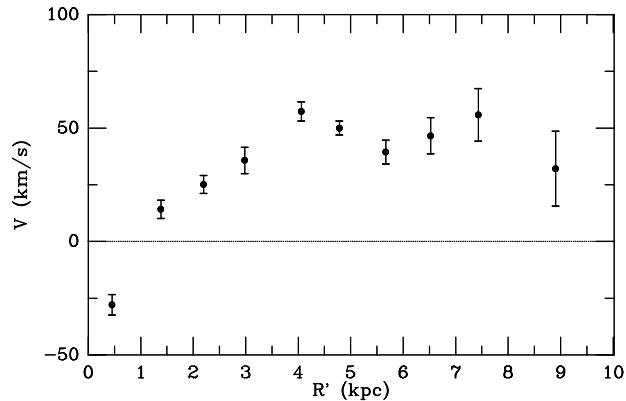


FIGURE 8. Rotation velocity  $V$  of carbon stars in the plane of the LMC disk as function of the cylindrical radius  $R'$  in kpc from the carbon star fits of van der Marel et al. (2002). For reference, the exponential disk scale length of the LMC is approximately 1.4 kpc.

When asymmetric drift is corrected for, the circular velocity in the disk plane can be calculated to be  $V_{\text{circ}} = 64.8 \pm 15.9 \text{ km s}^{-1}$ . The implied total mass of the LMC inside the last measured data point is therefore  $M_{\text{LMC}}(8.9 \text{ kpc}) = (8.7 \pm 4.3) \times 10^9 M_{\odot}$ . By contrast, the total stellar mass of the LMC disk is  $\sim 2.7 \times 10^9 M_{\odot}$  and the mass of the neutral gas in the LMC is  $\sim 0.5 \times 10^9 M_{\odot}$  (Kim et al. 1998). The combined mass of the visible material in the LMC is therefore insufficient to explain the dynamically inferred mass. The LMC must therefore be embedded in a dark halo. This is consistent with the fact that the observed rotation curve amplitude is relatively flat as a function of radius. The LMC tidal radius can be calculated to be  $r_t = 15.0 \pm 4.5 \text{ kpc}$ , which corresponds to an angle on the sky of  $17.1^{\circ} \pm 5.1^{\circ}$ . The uncertainty in the tidal radius is due primarily to our ignorance of how far the LMC dark halo extends. Either way, the tidal radius extends beyond the region for which most observations of the main body of the LMC are available. However, it should be kept in mind that the tidal radius marks the position beyond which material becomes unbound. The structure of a galaxy can be altered well inside of this radius (Weinberg 2000).

As discussed in Section 5.1, the line-of-sight velocity field constrains the value of  $w_{ts} = v_{ts} + D_0(di/dt)$ . The carbon stars yield  $w_{ts} = -402.9 \pm 13.0 \text{ km s}^{-1}$ . Given our knowledge of the proper motion and distance of the LMC (see Section 4) this implies that  $di/dt = -0.37 \pm 0.22 \text{ mas yr}^{-1} = -103 \pm 61 \text{ degrees/Gyr}$ . The LMC is the first galaxy for which it has been possible to measure  $di/dt$ . The  $N$ -body simulations by Weinberg (2000) show that the tidal torques from the Milky Way are expected to induce precession and nutation in the symmetry axis of the LMC disk plane. Although a detailed data-model comparison is not possible at the present time, it is comforting to note that the observed  $di/dt$  is of the same order as the rate of change of the disk orientation seen in the simulations.

### 5.3. HI Kinematics

HI gas provides another powerful method to study the kinematics of the LMC. High quality data is available from, e.g., Kim et al. (1998). Unfortunately, the kinematical analysis presented by Kim et al. was not as general as that discussed above for carbon stars. They did not leave  $w_{ts}$  as a free parameter in the fit. Instead, they corrected their data at the outset for the transverse motion of the LMC using the proper motion measured by Jones et al. (1994),  $(\mu_W, \mu_N) = (-1.37 \pm 0.28, -0.18 \pm 0.27) \text{ mas yr}^{-1}$ , and

assumed that  $di/dt = 0$ . This fixes  $w_{ts} = -175 \pm 72 \text{ km s}^{-1}$ , which is inconsistent with the value inferred from the carbon star velocity field. Kim et al. obtained a kinematic line of nodes that is both twisting with radius and inconsistent with the value determined from the carbon stars. In addition, they inferred a rotation curve for which the amplitude exceeds that in Figure 8 by  $\sim 40\%$ . It is likely that these results are affected by the imposed value of  $w_{ts}$ . A more general analysis of the HI kinematics is therefore desirable, but unfortunately, is not currently available. The same limitations apply to many of the other published studies of LMC tracer kinematics cited at the start of Section 5.

Independent of how the data are analyzed, it is likely that collisionless tracers provide a more appropriate means to study the structure of the LMC using equilibrium models than does HI gas. The dynamical center of the carbon star velocity field is found to be consistent (to within the  $\sim 0.4^\circ$  per-coordinate errors) with both the center of the bar and the center of the outer stellar contours. However, it has long been known that the center of the HI rotation velocity field does not coincide with the center of the bar, and it also doesn't coincide with the center of the outer contours of the stellar distribution. It is offset from both by  $\sim 1$  kpc. This indicates that the HI gas may not be in equilibrium in the the gravitational potential. Added evidence for this comes from the fact that the LMC and the SMC are enshrouded in a common HI envelope, and that they are connected by a bridge of HI gas (see Figure 5). Even at small radii the LMC gas disk appears to be subject to tidal disturbances (see Figure 4) that may well affect the velocity field.

## 6. Viewing Angles

A disk that is intrinsically circular will appear elliptical in projection on the sky. The viewing angles of the disk (see Figure 6) are then easily determined: the inclination is  $i = \arccos(1 - \epsilon)$ , where  $\epsilon$  is the apparent ellipticity on the sky, and the line-of-nodes position angle  $\Theta$  is equal to the major axis position angle  $\text{PA}_{\text{maj}}$  of the projected body. The viewing angles of the LMC have often been estimated under this assumption, using the projected contours for many different types of tracers (de Vaucouleurs & Freeman 1973; Bothun & Thompson 1988; Schmidt-Kaler & Gochermann 1992; Weinberg & Nikolaev 2001; Lynga & Westerlund 1963; Kontizas et al. 1990; Feitzinger et al. 1977; Kim et al. 1998; Alvarez et al. 1987). However, it now appears that this was incorrect. The kinematics of carbon stars imply  $\Theta = 129.9^\circ \pm 6.0^\circ$  (see Section 5.2), whereas the near-IR morphology of the LMC implies  $\text{PA}_{\text{maj}} = 189.3^\circ \pm 1.4^\circ$  (see Section 2). The result that  $\Theta \neq \text{PA}_{\text{maj}}$  implies that the LMC cannot be intrinsically circular. The value of  $\text{PA}_{\text{maj}}$  is quite robust; studies of other tracers have yielded very similar results, although often with larger error bars. The result that  $\Theta \neq \text{PA}_{\text{maj}}$  therefore hinges primarily on our confidence in the inferred value of  $\Theta$ . There have been other kinematical studies of the line of nodes, in addition to that described in Section 5.2. These have generally yielded values of  $\Theta$  that are both larger and twisting with radius (e.g., Kim et al. 1998; Alves & Nelson 2000). However, the accuracy of these results is suspect because of the important simplifying assumptions that were made in the analyses (see Section 5.3). No allowance was made for a potential solid-body rotation component in the velocity field due to precession and nutation of the LMC disk, which is both predicted theoretically (Weinberg 2000) and implied observationally by the carbon star data (see Section 5.2).

Arguably the most robust way to determine the LMC viewing angles is to use geometrical considerations, rather than kinematical ones. For an inclined disk, one side will be closer to us than the other. Tracers on that one side will appear brighter than similar tracers on the other side. This method does not rely on absolute distances or magnitudes, which are notoriously difficult to estimate, but only on relative distances or magnitudes.

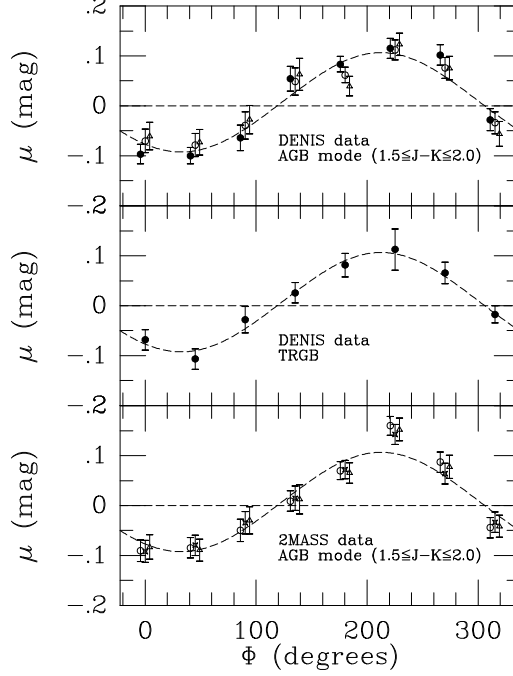


FIGURE 9. Variations in the magnitude of tracers as function of position angle  $\Phi$  from van der Marel & Cioni (2001). (a) Modal magnitude of AGB stars in the DENIS data with colors  $1.5 \leq J - K_s \leq 2.0$ . (b) TRGB magnitude from DENIS data. (c) As (a), but using data from the 2MASS Point Source Catalog. All panels refer to an annulus of radius  $2.5^\circ \leq \rho \leq 6.7^\circ$  around the LMC center. Filled circles, open circles, four-pointed stars and open triangles refer to the  $I$ ,  $J$ ,  $H$  and  $K_s$ -band, respectively. Results in different bands are plotted with small horizontal offsets to avoid confusion. The dashed curve shows the predictions for an inclined disk with viewing angles  $i = 34.7^\circ$  and  $\Theta = 122.5^\circ$ .

To lowest order, the difference in magnitude between a tracer at the galaxy center and a similar tracer at a position  $(\rho, \Phi)$  in the disk (as defined in Section 5.1) is

$$\mu = \left( \frac{5\pi}{180 \ln 10} \right) \rho \tan i \sin(\Phi - \Theta), \quad (6.1)$$

where the angular distance  $\rho$  is expressed in degrees. The constant in the equation is  $(5\pi)/(180 \ln 10) = 0.038$  magnitudes. Hence, when following a circle on the sky around the galaxy center one expects a sinusoidal variation in the magnitudes of tracers. The amplitude and phase of the variation yield estimates of the viewing angles  $(i, \Theta)$ .

Van der Marel & Cioni (2001) used a polar grid on the sky to divide the LMC area into several rings, each consisting of a number of azimuthal segments. The data from the DENIS and 2MASS surveys were used for each segment to construct near-IR CMDs similar to that shown in Figure 1. For each segment the modal magnitude (magnitude where the luminosity function peaks) was determined for carbon-rich AGB stars selected by color, as had been suggested by Weinberg & Nikolaev (2001). Figure 9 shows the inferred variation in magnitude as function of position angle  $\Phi$  for the radial range  $2.5^\circ \leq \rho \leq 6.7^\circ$ . The expected sinusoidal variations are confidently detected. The top panel shows the results for stars selected from the DENIS survey with the color selection criterion  $1.5 \leq J - K \leq 2.0$ . The bottom panel shows the results from the 2MASS survey

with the same color selection. The same sinusoidal variations are seen, indicating that there are no relative calibration problems between the surveys. Also, the same variations are seen in the  $I$ ,  $J$ ,  $H$  and  $K_s$  bands, which implies that the results are not influenced significantly by dust absorption. The middle panel shows the variations in the TRGB magnitudes as a function of position angle, from the DENIS data. RGB stars show the same variations as the AGB stars, suggesting that the results are not influenced significantly by potential peculiarities associated with either of these stellar populations. The observed variations can therefore be confidently interpreted as a purely geometrical effect. The implied viewing angles are  $i = 34.7^\circ \pm 6.2^\circ$  and  $\Theta = 122.5^\circ \pm 8.3^\circ$ . The  $\Theta$  value thus inferred geometrically is entirely consistent with the value inferred kinematically (see Section 5.2). Moreover, there is an observed drift in the center of the LMC isophotes at large radii which is consistent with both estimates, when interpreted as a result of viewing perspective (van der Marel 2001).

The aforementioned analyses are sensitive primarily to the structure of the outer parts of the LMC. Several other studies of the viewing angles have focused mostly on the region of the bar, which samples only the central few degrees. Many of these studies have been based on Cepheids. Their period-luminosity relation allows calculation of the distance to each individual Cepheid from a light curve. The relative distances of the Cepheids in the sample can then be analyzed in similar fashion as discussed above to yield the LMC viewing angles. Cepheid studies in the 1980s didn't have many stars to work with. Caldwell & Coulson (1986) analyzed optical data for 73 Cepheids and obtained  $i = 29^\circ \pm 6^\circ$  and  $\Theta = 142^\circ \pm 8^\circ$ . Laney & Stobie (1986) obtained  $i = 45^\circ \pm 7^\circ$  and  $\Theta = 145^\circ \pm 17^\circ$  from 14 Cepheids, and Welch et al. (1987) obtained  $i = 37^\circ \pm 16^\circ$  and  $\Theta = 167^\circ \pm 42^\circ$  from 23 Cepheids, both using near-IR data. The early Cepheid studies have now all been superseded by the work of Nikolaev et al. (2004). They analyzed a sample of more than 2000 Cepheids with lightcurves from MACHO data. Through use of photometry in five different bands, including optical MACHO data and near-IR 2MASS data, each star could be individually corrected for dust extinction. From a planar fit to the data they obtained  $i = 30.7^\circ \pm 1.1^\circ$  and  $\Theta = 151.0^\circ \pm 2.4^\circ$ . Other recent work has used the magnitude of the Red Clump to analyze the relative distances of different parts of the LMC. Olsen & Salyk (2002) obtained  $i = 35.8^\circ \pm 2.4^\circ$  and  $\Theta = 145^\circ \pm 4^\circ$ , also from an analysis that was restricted mostly to the inner parts of the LMC.

There is one caveat associated with all viewing angle results for the central few degrees of the LMC. Namely, it appears that the stars in this region are not distributed symmetrically around a single well-defined plane, as discussed in detail in Section 8.4. In the present context we are mainly concerned with the influence of this on the inferred viewing angles. Olsen & Salyk (2002) perform their viewing angle fit by ignoring fields south-west of the bar, which do not seem to agree with the planar solution implied by their remaining fields. By contrast, Nikolaev et al. (2004) fit all the stars in their sample, independent of whether or not they appear to be part of the main disk plane. Clearly, the  $(i, \Theta)$  results of Olsen & Salyk and Nikolaev et al. are the best-fitting parameters of well-posed problems. However, it is somewhat unclear whether they can be assumed to be unbiased estimates of the actual LMC viewing angles. For a proper understanding of this issue one would need to have both an empirical and a dynamical understanding of the nature of the extra-planar structures in the central region of the LMC. Only then is it possible to decide whether the concept of a single disk plane is at all meaningful in this region, and which data should be included or excluded in determining its parameters. This is probably not an issue for the outer parts of the LMC, given that the AGB star results of van der Marel & Cioni (2001) provide no evidence for extra-planar structures at radii  $\rho \geq 2.5^\circ$ .

In summary, all studies agree that  $i$  is in the range  $30^\circ$ – $40^\circ$ . At large radii,  $\Theta$  appears to be in the range  $115^\circ$ – $135^\circ$ . By contrast, at small radii all studies indicate that  $\Theta$  is in the range  $140^\circ$ – $155^\circ$ . As mentioned, it is possible that the results at small radii are systematically in error due to the presence of out-of-plane structures. Alternatively, it is quite well possible that there are true radial variations in the LMC viewing angles due to warps and twists of the disk plane. Many authors have suggested this as a plausible interpretation of various features seen in LMC datasets (van der Marel & Cioni 2001; Olsen & Salyk 2002; Subramaniam 2003; Nikolaev et al. 2004). Moreover, numerical simulations have shown that Milky Way tidal effects can drive strong warps in the LMC disk plane (Mastropietro et al. 2004).

## 7. Ellipticity

The inferred LMC viewing angles can be used to deproject the observed morphology that is seen in projection on the sky (van der Marel 2001). This yields an in-plane ellipticity  $\epsilon$  in the range  $\sim 0.2$ – $0.3$ , depending somewhat on the adopted viewing angles; e.g., the Nikolaev et al. (2004) angles give  $\epsilon = 0.21$  and the van der Marel & Cioni (2001) angles give  $\epsilon = 0.31$ . The conclusion that the LMC is elongated is in itself not surprising. The dark matter halos predicted by cosmological simulations are generally triaxial (e.g., Dubinski & Carlberg 1991), and the gravitational potential in the equatorial plane of such halos does not have circular symmetry. So it is generally expected that disk galaxies are elongated rather than circular. Furthermore, it is possible to construct self-consistent dynamical models for elliptical disks (e.g., Teuben 1987). What is surprising is that the LMC ellipticity is fairly large. Studies of the apparent axis ratio distribution of spiral galaxy disks (Binney & de Vaucouleurs 1981; Lambas, Maddox & Loveday 1992) of the structure of individual spiral galaxies (Rix & Zaritsky 1995; Schoenmakers, Franx & de Zeeuw 1997; Kornreich, Haynes & Lovelace 1998; Andersen et al. 2001) and of the scatter in the Tully-Fisher relation (Franx & de Zeeuw 1992) indicate that the average (deprojected) ellipticity of spiral galaxies is only 5–10%. So while spiral galaxies are generally elongated, their elongation is usually smaller than inferred here for the LMC. Of course, galaxies of type Sm and Im are (by definition) more irregular and lopsided than spirals. So it is not a priori clear whether or not the LMC is atypically elongated for its Hubble type.

It is interesting to ask what may be the cause of the large in-plane ellipticity of the LMC. The prime candidate is distortion by the Milky Way tidal field. The present-day tidal force on the LMC by the Milky Way exceeds that from the SMC. Moreover, the Milky Way tidal field is responsible for other well-known features of the Magellanic system, such as the Magellanic Stream (see Section 3). N-body simulations have shown that the structure of the LMC can be altered significantly by the Milky Way tidal force (Weinberg 2000) and the simulations of Mastropietro et al. (2004) indeed predict a considerable in-plane elongation for the LMC. Also, the LMC elongation in projection on the sky points approximately towards the Galactic Center and is perpendicular to the Magellanic Stream (van der Marel 2001), as predicted naturally by simulations of tidal effects (Mastropietro et al. 2004). However, a very detailed data-model comparison is not possible at the present time. That would require accurate knowledge of the past history as a function of time of the LMC orbit, of the disk-plane orientation due to precession and nutation, and of the LMC-SMC distance. Such knowledge is not available at the present time.

A consequence of the ellipticity of the LMC disk is that one cannot expect the streamlines of tracers in the disk to be perfectly circular, by contrast to what has been assumed



in all kinematical studies to date. The effect of this is probably not large, because the gravitational potential of a mass distribution is always rounder than the mass distribution itself. One effect of ellipticity is an apparent offset between the kinematical line of nodes and the true line of nodes (Schoenmakers, Franx & de Zeeuw 1997). This effect is presently not at observable levels, given that kinematical analysis of carbon stars (see Section 5) yields a line-of-nodes position angle  $\Theta$  that is in adequate agreement with geometrical determinations (see Section 6). However, it should be kept in mind that, as the sophistication of the studies of LMC kinematics increases, it might become necessary to account for the effect of non-circularity on the observed kinematics.

## 8. Vertical Structure and Microlensing

### 8.1. Scale Height

The scale height of the LMC disk can be estimated from the observed line-of-sight velocity dispersion  $\sigma$ . For carbon stars, the scatter of the velocity measurements around the best-fitting rotating disk model (Figure 7) yields  $\sigma = 20.2 \pm 0.5 \text{ km s}^{-1}$ . The ratio of rotation velocity to velocity dispersion is therefore  $V/\sigma = 2.9 \pm 0.9$ . For comparison, the thin disk of the Milky Way has  $V/\sigma \approx 9.8$  and its thick disk has  $V/\sigma \approx 3.9$ . In a relative sense one might therefore expect the LMC disk to be similar, but somewhat thicker than the Milky Way thick disk. Weinberg (2000) argued from  $N$ -body simulations that such considerable thickness could be the result of Milky Way tidal effects on the LMC.

The radial profile of the velocity dispersion contains information on the LMC scale height as function of radius. The carbon star velocity dispersion is close to constant as function of radius, and this is not what is expected for a disk with a constant scale height. To fit this behavior one must assume that the scale height increases with radius in the disk (Alves & Nelson 2000). This can arise naturally as a result of tidal forces from the Milky Way, which become relatively more important (compared to the LMC self-gravity) as one moves to larger radii. Alves & Nelson considered an isothermal disk with a vertical density profile proportional to  $\text{sech}^2(z/z_0)$ , where  $z_0$  can vary with disk radius. Application to the carbon star data of van der Marel et al. (2002) yields  $z_0 = 0.27 \text{ kpc}$  at the LMC center, rising to  $z_0 = 1.5 \text{ kpc}$  at a radius of  $5.5 \text{ kpc}$ .

The LMC carbon stars are part of the intermediate-age population which is believed to be fairly representative for the bulk of the mass in the LMC. In this sense, the results inferred for the carbon star population are believed to be characteristic for the LMC as a whole. However, it is certainly not true that all populations have the same kinematics. As in the Milky Way, younger populations have a smaller velocity dispersion (and hence a smaller scale height) than older populations. A summary of measurements for various populations is given by Gyuk, Dalal & Griest (2000). The youngest populations (e.g., supergiants, HII regions, HI gas) have dispersions of only  $\sigma \approx 6 \text{ km s}^{-1}$ . Old long-period variables have dispersions  $\sigma \approx 30 \text{ km s}^{-1}$  (Bessell, Freeman & Wood 1986) and so do the oldest star clusters (Freeman et al. 1983; Schommer et al. 1992). These values are considerably below the LMC circular velocity (see Section 5.2). This has generally been interpreted to mean that the LMC does not have an old pressure supported halo similar to that of the Milky Way.

The first possible evidence for the presence of a pressure supported halo was presented recently by Minniti et al. (2003). They measured a dispersion  $\sigma \approx 53 \pm 10 \text{ km s}^{-1}$  for a sample of 43 RR Lyrae stars within  $1.5^\circ$  from the LMC center. This value is consistent with what would be expected for a pressure supported halo in equilibrium in the gravitational potential implied by the circular velocity (Alves 2004a). The RR Lyrae stars make

up  $\sim 2\%$  of the visible mass of the LMC, similar to the value for the Milky Way halo. However, it is surprising that the surface density distribution of the LMC RR Lyrae stars is well fit by an exponential with the same scale length as inferred for other tracers known to reside in the disk (Alves 2004a). This is very different from the situation for the Milky Way halo, where RR Lyrae stars follow a power-law density profile. This suggests that maybe the RR Lyrae stars in the LMC did form in the disk, instead of in a halo. In this scenario they might simply have attained their large dispersions by a combination of disk heating and Milky Way tidal forces (Weinberg 2000). To discriminate between halo and disk origins it will be important to determine whether the velocity field of the RR Lyrae stars has a rotation component. This will require observations at larger galactocentric distances.

### 8.2. *Microlensing Optical Depth*

One of the most important reasons for seeking to understand the vertical structure of the LMC is to understand the results from microlensing surveys. The observed microlensing optical depth towards the LMC is  $\tau_{\text{obs}} = 12_{-3}^{+4} \times 10^{-8}$  with an additional 20–30% of systematic error (Alcock et al. 2000a). It has generally been found that equilibrium models for the LMC do not predict enough LMC self-lensing events to account for the observed optical depth (Gyuk, Dalal & Griest 2000; Jetzer, Mancini & Scarpetta 2002). For the most favored set of LMC model parameters in the Gyuk et al. study the predicted self-lensing optical depth is  $\tau_{\text{self}} = 2.2 \times 10^{-8}$ , a factor of 5.5 less than the observed value. To account for the lenses it is therefore necessary to assume that some  $\sim 20\%$  of the Milky Way dark halo is made up of lenses of mass  $0.15\text{--}0.9M_{\odot}$  (Alcock et al. 2000a). However, it is a mystery what the composition of this lensing component could be. A large population of old white dwarfs has been suggested, but this interpretation is not without problems (e.g., Fields, Freese, & Graff 2000; Flynn, Holopainen, & Holmberg 2003). It is therefore worthwhile to investigate whether the models that have been used to estimate the LMC self-lensing might have been oversimplified. This is particularly important since there is evidence from the observed microlensing events themselves that many of the lenses may reside in the LMC (Sahu 2003).

To lowest order, the self-lensing optical depth in simple disk models of the LMC depends exclusively on the observed velocity dispersion and not separately on either the galaxy mass or scale height (Gould 1995). One way to increase the self-lensing predicted by LMC models is therefore to assume that a much larger fraction of the LMC mass resides in high velocity dispersion populations than has previously been believed. Salati et al. (1999) showed that the observed optical depth can be reproduced if one assumes that 70% of the mass in the LMC disk consists of objects with  $\sigma$  ranging from  $25 \text{ km s}^{-1}$  to  $60 \text{ km s}^{-1}$ . However, this would seem difficult to explain on the basis of present data. Although RR Lyrae stars have now been observed to have a high velocity dispersion, these old stars make up only 2% of the visible mass. So their influence on self-lensing predictions is negligible. A better way to account for the observed optical depth might be to assume that the vertical structure of the LMC is more complicated than for normal disk galaxies. The self-lensing optical depth might then have been considerably underestimated.

### 8.3. *Foreground and Background Populations*

One way to explain the observed microlensing optical depth is to assume that there might be stellar populations outside of the main LMC disk plane. For example, there might be a population of stars in front of or behind the LMC that was pulled from the Magellanic Clouds due to Milky Way tidal forces (Zhao 1998) or there might be a non-virialized shroud of stars at considerable distances above the LMC plane due to Milky Way tidal heating (Weinberg 2000; Evans & Kerins 2000). If microlensing source

stars belong to such populations, then this would yield observable signatures in their characteristics. In particular, if microlensing source stars are behind the LMC, then they should be systematically fainter (Zhao, Graff & Guhathakurta 2000) and redder (Zhao 1999, 2000) than LMC disk stars. HST/WFPC2 CMDs of fields surrounding microlensing events show no evidence for this, although the statistics are insufficient to rule out specific models with strong confidence (Alcock et al. 2001). Other tests of the spatial distribution and properties of the LMC microlensing events also do not (yet) discriminate strongly between different models for the location and nature of either the lenses or the sources (Alcock et al. 2000a; Gyuk, Dalal & Griest 2000; Jetzer, Mancini & Scarpetta 2002). This is primarily because only 13–17 LMC microlensing events are known. So to assess whether the LMC has out-of-plane structures it is best to focus on other types of tracers that might yield better statistics.

Zaritsky & Lin (1997) studied the optical CMD of a field  $\sim 2^\circ$  north-west of the LMC center and found a vertical extension at the bright end of the Red Clump. They suggested that this feature is due to stars 15–17 kpc above the LMC disk. However, this interpretation has been challenged for many different reasons (e.g., Bennett 1998; Gould 1998, 1999). Most seriously, Beaulieu & Sackett (1998) pointed out that a Vertical Red Clump (VRC) extension is naturally expected from stellar evolution due to young helium core burning stars. The same feature is seen in the Fornax and Sextans A dwarfs (Gallart 1998). It remains somewhat open to discussion whether the number of stars in the LMC VRC is larger than expected given our understanding of the LMC star formation history, so a foreground population is not strictly ruled out (Zaritsky et al. 1999). However, it certainly doesn't appear to be a favored interpretation of the data. Also, the kinematics of the VRC stars is indistinguishable from that of LMC Red Clump stars (Ibata, Lewis & Beaulieu 1998). More recently, Zhao et al. (2003) performed a detailed radial velocity survey of 1300 stars of various types within  $\sim 2^\circ$  from the LMC center. They found no evidence for stars with kinematics that differ significantly from that of the main LMC disk. This rules out a significant foreground or background population of stars that reside in a tidal stream that is seen superposed onto the LMC by chance (Zhao 1999). Any foreground or background population must be physically associated with the LMC, and share its kinematics. Sub-populations within the LMC with subtly different kinematics have been suggested (Graff et al. 2000), but only at low statistical significance.

Other arguments for stars at large distances from the LMC disk also have not been convincing. Kunkel et al. (1997b) argued on the basis of carbon star velocities that the LMC has a polar ring. However, the carbon star velocity field shown in Figure 7 seems to be well fit by a single rotation disk model. It is possible that the Kunkel et al. study was affected by the use of an LMC transverse velocity value of only  $240 \text{ km s}^{-1}$ , which is considerably below the value indicated by presently available proper motion data ( $406 \pm 44 \text{ km s}^{-1}$ ; see Section 4). Weinberg & Nikolaev (2001) found a tail of relatively faint stars in luminosity functions of AGB stars selected by  $J-K$  color from 2MASS data. They suggested that this is not due to dust extinction but might indicate stars behind the LMC. On the other hand, the distribution of these stars on the sky (van der Marel, unpublished) bears a strong resemblance to the far infrared IRAS map of LMC dust emission (Schwering 1989). This casts doubt on the interpretation that the brightnesses of these stars have not been affected by dust. Weinberg & Nikolaev (2001) also found a slightly non-Gaussian tail in their AGB star luminosity functions towards brighter magnitudes. However, this need not indicate stars in the foreground, given that there is no a priori reason why the AGB star luminosity function would have to be Gaussian. In another study, Alcock et al. (1997) found no evidence for unexpected numbers of RR Lyrae stars at distances beyond  $\sim 15$  kpc from the LMC disk plane.

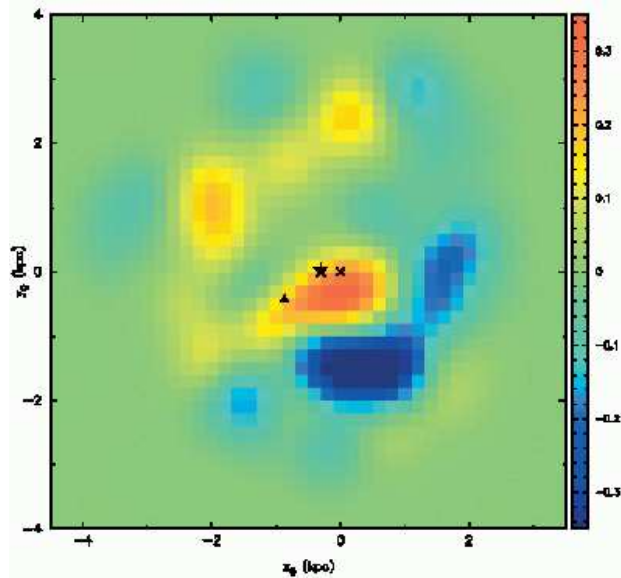


FIGURE 10. Map of the average vertical distances of Cepheids (in kpc) from a best-fitting plane solution as function of in-plane coordinates  $(x_0, y_0)$  from Nikolaev et al. (2004). The orientation of the bar in this representation is similar as in Figure 2. Negative (positive) distances denote material behind (in front of) the fitted plane. The cross indicates the HI rotation center according to Kim et al. (1998), the star shows the geometric center of the Cepheid sample, and the triangle gives the center of the outer carbon star isophotes from van der Marel & Cioni (2001). A color version of the image is available in the Nikolaev et al. paper.

#### 8.4. Non-planar Structure in the LMC Disk

The studies discussed in Sections 5 and 6 indicate that the overall structure of the LMC is that of a (thick) disk. From Section 8.3 it follows that there is no strong evidence for unexpected material far from the disk plane. However, this does not mean that there may not be non-planar structures in the disk itself. For example, it was already discussed in Section 6 that there might be warps and twists in the disk plane.

Early evidence for non-planar material came from HI observations. One of the most prominent optical features of the LMC is the star forming 30 Doradus complex, located just north of the eastern tip of the bar. This region is a very strong source of UV radiation, yet the HI gas disk of the LMC does not show a void in this part of the sky. This indicates that the 30 Doradus complex cannot be in the plane of the LMC disk, but must be at least 250–400 kpc away from it (Luks & Rohlfs 1992). HI channel maps show that there is a separate HI component, called the “L-component”, that is distinct from the main LMC disk. It has lower line-of-sight velocities than the main disk by 20–30  $\text{km s}^{-1}$ , contains some 19% of the HI gas in the LMC, and does not extend beyond  $2^\circ$ – $3^\circ$  from the LMC center (Luks & Rohlfs 1992). Absorption studies indicate that this component is behind the LMC disk (Dickey et al. 1994). The 30 Doradus complex is spatially located at the center of the L-component. It is probably directly associated with it, given that the L-component shows a hole of HI emission at the 30 Doradus position as expected from ionization. These results suggest that in the central few degrees of the LMC an important fraction of the gas and stars may not reside in the main disk.

It has now proven possible to test some of these ideas more directly by using large stellar databases. Section 6 already mentioned the study of more than 2000 Cepheids by

Nikolaev et al. (2004). They obtained accurate reddening-corrected (relative) distances to each of the Cepheids. The distance residuals with respect to the best-fitting plane do not follow a random Gaussian distribution. Instead they show considerable structure, as shown in Figure 10. The two-dimensional distribution of the residuals on the sky was interpreted as a result of two effects, namely a symmetric warp in the disk, and the fact that the bar is located  $\sim 0.5$  kpc in front of the main disk. Interestingly, an offset between the LMC bar and disk had previously been suggested by Zhao & Evans (2000) as an explanation for the observed LMC microlensing optical depth. If the disk and the bar of the LMC are not dynamically connected, then this may also explain why in projection the LMC bar appears offset from the center of the outer isophotes.

The variation of the reddening-corrected Red Clump magnitude over the face of the LMC has also been used to study vertical structures in the LMC disk. Olsen & Salyk observed 50 randomly selected fields in the central  $4^\circ$  of the LMC at CTIO. They found that fields between  $2^\circ$ – $4^\circ$  south-west of the LMC center are 0.1 mag brighter than expected from the best plane fit. They interpreted this to indicate that stars in these fields lie some 2 kpc above the LMC disk, and argued for warps and twists in the LMC disk plane. Subramaniam (2003) used Red Clump magnitudes determined from stars in the OGLE database to address the same issue. This yielded a map of the Red Clump magnitude along the length and width of the LMC bar. This map shows considerable structure and clearly cannot be fit as a single plane. Subramaniam (2004) suggested that the residuals can be interpreted as the result of a misaligned secondary bar inside the primary bar.

Eclipsing binaries have also provided interesting information on this subject. These binaries can be modeled in detail to yield a fairly accurate distance. The distances of sources studied so far seem to indicate a slightly lower LMC distance modulus of  $m - M \approx 18.4$  (Ribas et al. 2002) than has been inferred from other tracers (see Section 4). However, it is possible to obtain somewhat higher values with a slightly different analysis (Groenewegen & Salaris 2001; Clausen et al. 2003) so this is no great cause for concern (Alves 2004b). What is interesting though is that four eclipsing binaries analyzed by the same team with the same method show a considerable spread in distance. This has been interpreted to mean that one of the binaries lies  $\sim 3$  kpc behind the LMC disk plane (Ribas et al. 2002) and that another one lies  $\sim 4$  kpc in front of it (Fitzpatrick et al. 2003).

The above studies indicate that there is considerable and complicated vertical structure in the central few degrees of the LMC disk. However, this is a rapidly developing field, and many important questions remain open. In particular, it is unclear whether the features reported in the various studies are actually the same or not. Qualitative comparison is not straightforward. Different authors study different areas of the LMC, they plot residuals with respect to different planes, and they present their results in figures that plot different types of quantities. However, cursory inspection of the various papers shows very few features that are obviously in common between the studies. Quantitative comparison is therefore needed. Direct comparison to the results for the outer parts of the LMC, where there is little evidence for extra-planar structures (van der Marel & Cioni 2001), is also important. If discrepancies emerge from such comparisons, then this can mean two things. Either some studies are in error (e.g., due to use of inaccurate dust corrections, or by incorrect interpretation of stellar evolutionary variations as distance variations) or different tracers do not trace the same structure. The latter might well be the case. Cepheids are young stars with ages less than a few times  $10^8$  years whereas stars on the RGB and AGB are typically older than 1 Gyr. Since the structure of the LMC and its gaseous component vary with time as a result of tidal interactions with the Milky Way and the

SMC, one wouldn't necessarily expect stars formed at different epochs to trace identical structures.

Another open question is what the physical and dynamical interpretation is of the extra-planar structures that are being detected. Many authors have used the term “warp”. However, the residuals that have been reported do not much resemble the smoothly varying residuals that are expected from a single plane with a global warp. The structures appear to be both different and more complicated than a single warp. If a decomposition into different components is attempted, then such a decomposition must use entities that can be understood dynamically (disk, bar, bulge, warp, etc.) and that make sense in the context of the overall evolutionary history of the Magellanic System. Components with holes or sharp edges (e.g., Subramaniam 2004) are not particularly realistic from a dynamical viewpoint. Phase mixing of stellar orbits quickly removes such sharp discontinuities. Also, if the vertical structures detected in the inner region of the LMC disk are due to components that are not connected to the main disk plane, then why does the projected image of the LMC (e.g., Figure 2) look so smooth? And why is there so little evidence from stellar kinematics for components with decoupled kinematics (e.g., Figure 7; Zhao et al. 2003)? Clearly, many questions remain to be answered before we can come to a full understanding of the vertical structure of the LMC.

## 9. Concluding Remarks

The structure and kinematics of the LMC continue to be active areas of research. As outlined in this review, much progress has been made recently. Improved datasets have played a key role in this, most notably the advent of large stellar datasets of magnitudes in many bands, lightcurves, and line-of-sight kinematics, and also the availability of sensitive HI observations over large areas. As a result we now have a fairly good understanding of the LMC morphology and kinematics. The proper motion of the LMC is reasonably well measured and the global properties of the LMC orbit around the Milky Way are understood. The angles that determine how we view the LMC are now known much more accurately than before and this has led to the realization that the LMC is quite elliptical in its disk plane. We are starting to delineate the vertical structure of the LMC and are finding complexities that were not previously expected.

Despite the excellent progress, many questions on LMC structure still remain open. Why is the bar offset from the center of the outer isophotes of the LMC? Why is the dynamical center of the HI offset from the center of the bar, from the center of the outer isophotes, and from the dynamical center of the carbon stars? Why do studies of the inner and outer regions of the LMC yield differences in line-of-nodes position angle of up to  $30^\circ$ ? Does the LMC have a pressure supported halo? Are there populations of stars at large distances from the LMC plane? What is the origin and dynamical nature of the non-planar structures detected in the inner regions of the LMC? Do different tracers outline the same non-planar structures?

It might be necessary to answer all of these open questions before we can convince ourselves that the optical depth for LMC self-lensing has been correctly estimated. This seems to be the most critical step in establishing whether or not the Milky Way halo contains hitherto unknown compact lensing objects (MACHOs). The open questions about LMC structure are important also in their own right. The tidal interaction between the Magellanic Clouds and the Milky Way provides one of our best laboratories for studying the processes of tidal disruption and hierarchical merging by which all galaxies are believed to grow. A better understanding of LMC structure may also provide new insight into the origin of the Magellanic Stream, which continues to be debated. And

with improved proper motion measurements of the Magellanic Clouds, the Stream may become a unique tool to constrain the shape and radial density distribution of the Milky Way halo at radii inaccessible using other tracers.

## REFERENCES

- Alcock, C., et al. 1997, *ApJ*, 490, L59  
Alcock, C., et al. 2000a, *ApJ*, 542, 281  
Alcock, C., et al. 2000b, *AJ*, 119, 2194  
Alcock, C., et al. 2001, *ApJ*, 552, 582  
Alvarez, H., Aparici, J., & May, J. 1987, *A&A*, 176, 25  
Alves, D. R. 2004a, *ApJ*, 601, L151  
Alves, D. R. 2004b, in *Highlights of Astronomy*, Vol. 13, O. Engvold, ed., in press (Elsevier) [astro-ph/0310673]  
Alves, D. R., & Nelson, C. A. 2000, *ApJ*, 542, 789  
Andersen, D. R., Bershady, M. A., Sparke, L. S., Gallagher III, J. S., & Wilcots, E. M. 2001, *ApJ*, 551, L131  
Anguita, C., Loyola, P., & Pedreros, M. H. 2000, *AJ*, 120, 845  
Beaulieu, J.-P., & Sackett, P. D. 1998, *AJ*, 116, 209  
Bennett, D. P. 1998, *ApJ*, 493, L79  
Bessell, M. S., Freeman, K. C., & Wood, P. R. 1986, *ApJ*, 310, 710  
Binney, J. J., & de Vaucouleurs, G. 1981, *MNRAS*, 194, 679  
Bothun, G. D., & Thompson, I. B. 1988, *AJ*, 96, 877  
Caldwell, J. A. R., & Coulson, I. M. 1986, *MNRAS*, 218, 223  
Cioni, M. R., et al. 2000a, *A&AS*, 144, 235  
Cioni, M.-R. L., Habing, H. J., & Israel, F. P. 2000b, *A&A*, 358, L9  
Clausen, J. V., Storm, J., Larsen, S. S., & Gimenez, A. 2003, *A&A*, 402, 509  
Connors, T. W., Kawata, D., Maddison, S. T., & Gibson, B. K. 2004, *PASA*, in press [astro-ph/0402187]  
Crowl, H. H., Sarajedini, A., Piatti, A. E., Geisler, D., Bica, E., Claria, J. J., & Santos, J. F. C., Jr. 2001, *AJ*, 122, 220  
Delmotte, N., Loup, C., Egret, D., & Cioni, M.-R., Pierfederici, F. 2002, *A&A*, 396, 143  
de Vaucouleurs, G., & Freeman, K. C. 1973, *Vistas Astron.*, 14, 163  
Dickey, J. M., Mebold, U., Marx, M., Amy, S., Haynes, R. F., & Wilson, W. 1994, *A&A*, 289, 357  
Drake, A., et al. 2002, 199th Meeting of the American Astronomical Society, 52.05  
Dubinski, J., & Carlberg, R. G. 1991, *ApJ*, 378, 496  
Epchtein, N., et al. 1997, *Messenger*, 87, 27  
Evans, N. W., & Kerins, E. 2000, *ApJ*, 529, 917  
Feitzinger, J. V., Schmidt-Kaler, T., & Isserstedt, J. 1977, *A&A*, 57, 265  
Fields, B., Freese, K., & Graff, D. S. 2000, *ApJ*, 534, 265  
Fitzpatrick, E. L., Ribas, I., Guinan, E. F., Maloney, F. P., & Claret, A. 2003, *ApJ*, 587, 685  
Flynn, C., Holopainen, J., & Holmberg, J. 2003, *MNRAS*, 339, 817  
Franx, M., & de Zeeuw, P. T. 1992, *ApJ*, 392, L47  
Freedman, W. L., et al. 2001, *ApJ*, 553, 47  
Freeman, K. C., Illingworth, G., & Oemler, A. 1983, *ApJ*, 272, 488  
Gallart, C. 1998, *ApJ*, 495, L43  
Gardiner, L. T., & Noguchi, 1996, *MNRAS*, 278, 191  
Gardiner, L. T., Sawa, T., & Fujimoto, M. 1994, *MNRAS*, 266, 567  
Gibson, B. K. 2000, *Mem. Soc. Astron. Italiana* [astro-ph/9910574]  
Gould, A. 1995, *ApJ*, 441, 77  
Gould, A. 1998, *ApJ*, 499, 728  
Gould, A. 1999, *ApJ*, 525, 734  
Graff, D. S., Gould, A. P., Suntzeff, N. B., Schommer, R. A., & Hardy, E. 2000, *ApJ*, 540, 211

- Groenewegen, M. A. T., & Salaris, M. 2001, *A&A*, 366, 752
- Guhathakurta, P., & Reitzel, D. B. 1998, in *Galactic Halos: A UC Santa Cruz Workshop*, D. Zaritsky, ed., ASP Conference Series 136, p. 22
- Gyuk, G., Dalal, N., & Griest, K. 2000, *ApJ*, 535, 90
- Hatzidimitriou, D., Croke, B. F., Morgan, D. H., & Cannon, R. D. 1997, *A&AS*, 122, 507
- Heller, P., & Rohlfs, K. 1994, 291, 743
- Ibata, R. A., Lewis, G. F., & Beaulieu, J.-P. 1998, *ApJ*, 509, L29
- Ibata, R., Lewis, G. F., Irwin, M., Totten, E., & Quinn, T. 2001, *ApJ*, 551, 294
- Irwin, M. J. 1991, in *The Magellanic Clouds, Proceedings IAU Symposium 148*, R. Haynes, & D. Milne, p. 453 (Dordrecht: Kluwer Academic Publishers)
- Jetzer, P., Mancini, L., & Scarpitta, G. 2002, *A&A*, 393, 129
- Jones, B. F., Klemola, A. R., & Lin, D. N. C. 1994, *AJ*, 107, 1333
- Kim, S., Staveley-Smith, L., Dopita, M. A., Freeman, K. C., Sault, R. J., Kesteven M. J., & McConnell, D. 1998, *ApJ*, 503, 674
- Kim, S., Staveley-Smith, L., Dopita, M. A., Sault, R. J., Freeman, K. C., Lee, Y., & Chu, Y.-H. 2003, *ApJS*, 148, 473
- Kochanek, C. S. 1996, *ApJ*, 457, 228
- Kontizas, M., Morgan, D. H., Hatzidimitriou, D., & Kontizas, E. 1990, *A&AS*, 84, 527
- Kontizas, E., Dapergolas, A., Morgan, D. H., & Kontizas, M. 2001, *A&A*, 369, 932
- Kornreich, D. A., Haynes, M. P., & Lovelace, R. V. E. 1998, *AJ*, 116, 2154
- Kroupa, P., Röser, S., & Bastian, U. 1994, *MNRAS*, 266, 412
- Kroupa, P., & Bastian, U. 1997, *New Astronomy*, 2, 77
- Kunkel, W. E., Irwin, M. J., & Demers, S. 1997a, *A&AS*, 122, 463
- Kunkel, W. E., Demers, S., Irwin, M. J., & Albert, L. 1997b, *ApJ*, 488, L129
- Kunkel, W. E., Demers, S., & Irwin, M. J. 2000, *AJ*, 119, 2789
- Lambas, D. G., Maddox, S. J. & Loveday, J. 1992, *MNRAS*, 258, 404
- Laney, C. D., & Stobie, R. S. 1986, *MNRAS*, 222, 449
- Lin, D. C. N., Jones, B. F., & Klemola, A. R. 1995, *ApJ*, 439, 652
- Lin, D. N. C., & Lynden-Bell, D. 1982, *MNRAS*, 198, 707
- Liu, Y.-Z. 1992, *A&A*, 257, 505
- Lu, L., Sargent, W. L. W., Savage, B. D., Wakker, B. P., Sembach, K. R., & Oosterloo, T. A. 1998, *AJ*, 115, 162
- Luks, Th., & Rohlfs, K. 1992, *A&A*, 263, 41
- Lynga, G., & Westerlund, B. E. 1963, *MNRAS*, 127, 31
- Majewski, S. R., Skrutskie, M. F., Weinberg, M. D., & Ostheimer, J. C. 2003, *ApJ*, 599, 1082
- Maragoudaki, F., Kontizas, M., Morgan, D. H., Kontizas, E., Dapergolas, A., & Livanou, E. 2001, *A&A*, 379, 864
- Marigo, P., Girardi, L., & Chiosi, C. 2003, *A&A*, 403, 225
- Mastropietro, C., Moore, B., Mayer, L., & Stadel, J. 2004, in *Satellites and Tidal Streams*, F. Prada, D. Martinez-Delgado, & T. Mahoney, eds., ASP Conf. Series, in press [astro-ph/0309244]
- McGee, R. X., & Milton, J. A. 1966, *Austr. Journal of Physics*, 19, 343
- Meatheringham, S. J., Dopita, M. A., Ford, H. C., & Webster, B. L. 1988, *ApJ*, 327, 651
- Minniti, D., Borissova, J., Rejkuba, M., Alves, D. R., Cook, K. H., Freeman, K. C. 2003, *Science*, 301, 1508
- Moore, B., & Davis, M. 1994, *MNRAS*, 270, 209
- Murai, T., & Fujimoto, M. 1980, *PASJ*, 32, 581
- Nikolaev, S., & Weinberg, M. D. 2000, *ApJ*, 542, 804
- Nikolaev, S., Drake, A.J., Keller, S. C., Cook, K. H., Dalal, N., Griest, K., Welch, D. L., & Kanbur, S. M. 2004, 601, 260
- Olsen, K. A. G., & Salyk, C. 2002, *AJ*, 124, 2045
- Pedrerros, M. H., Anguita, C., & Maza, J. 2002, *AJ*, 123, 1971
- Putman, M. E., et al. 1998, *Nature*, 394, 752
- Putman, M. E., Staveley-Smith, L., Freeman, K. C., Gibson, B. K., & Barnes, D. G. 2003, *ApJ*, 586, 170



- Ribas, I., Fitzpatrick, E. L., Maloney, F. P., Guinan, E. F., & Udalski, A. 2002, *ApJ*, 574, 771
- Rix, H.-W., & Zaritsky, D. 1995, *ApJ*, 447, 82
- Rohlf, K., Kreitschmann, J., Siegman, B. C., & Feitzinger, J. V. 1984, *A&A* 137, 343
- Sahu, K. C. 2003, in *The Dark Universe: Matter, Energy, and Gravity*, M. Livio, ed., 14 (Cambridge: Cambridge University Press)
- Salati, P., Tallet, R., Aubourg, E., Palanque-Delabrouille, N., & Spiro, M. 1999, *A&A*, 350, L57
- Schmidt-Kaler, T., & Goehermann, J. 1992, in *Variable Stars and Galaxies*, B. Warner, ed., ASP Conf. Series Vol. 30, 203
- Schoenmakers, R. H. M., Franx, M., & de Zeeuw, P. T. 1997, *MNRAS*, 292, 349
- Schommer, R. A., Suntzeff, N. B., Olszewski, E. W., & Harris, H. C. 1992, *AJ*, 103, 447
- Schwering, P. B. W. 1989, *A&AS*, 99, 105
- Shuter, W. L. H. 1992, *ApJ*, 386, 101
- Skrutskie, M. 1998, in *The Impact of Near-Infrared Sky Surveys on Galactic and Extragalactic Astronomy*, Proc. of the 3rd Euroconference on Near-Infrared Surveys, N. Epchtein., ed., Astrophysics and Space Science Library, Vol. 230, 11 (Dordrecht: Kluwer)
- Stanimirovic, S., Staveley-Smith, L., Dickey, J. M., Sault, R. J., & Snowden, S. L. 1999, *MNRAS*, 302, 417
- Stanimirovic, S., Staveley-Smith, L., & Jones, P. 2004, *ApJ*, 604, 176
- Staveley-Smith, L., Kim, S., Calabretta, M. R., Haynes, R. F., & Kesteven, M. J. 2003, *MNRAS*, 339, 87
- Subramaniam, A. 2003, *ApJ*, 598, L19
- Subramaniam, A. 2004, *ApJ*, 604, L41
- Teuben, P. 1987, *MNRAS*, 227, 815
- Udalski, A., Szymanski, M., Kubiak, M., Pietrzynski, G., Wozniak, P., & Zebrun, K. 1998, *Acta Astronomica*, 48, 147
- Udalski, A., Szymanski, M., Kubiak, M., Pietrzynski, G., Soszynski, I., Wozniak, P., & Zebrun, K. 2000, *Acta Astronomica*, 50, 307
- van den Bergh, S. 2000, *The Galaxies of the Local Group* (Cambridge: Cambridge University Press)
- van der Marel, R. P., & Cioni, M.-R. 2001, *AJ*, 122, 1807
- van der Marel, R. P. 2001, *AJ*, 122, 1827
- van der Marel, R. P., Alves, D. R., Hardy, E., & Suntzeff, N. B. 2002, *AJ*, 124, 2639
- Weinberg, M. D. 2000, *ApJ*, 532, 922
- Weinberg, M. D., & Nikolaev, S. 2001, *ApJ*, 548, 712
- Welch, D. L., McLaren, R. A., Madore, B. F., & McAlary, C. W. 1987, *ApJ*, 321, 162
- Westerlund, B. E. 1997, *The Magellanic Clouds* (Cambridge: Cambridge University Press)
- Wilkinson, M. I., & Evans, N. W. 1999, *MNRAS*, 310, 645
- Yoshizawa, A. M., & Noguchi, M. 2003, *MNRAS*, 339, 1135
- Zaritsky, D. 1999, *AJ*, 118, 2824
- Zaritsky, D., Harris, J., & Thompson, I. 1997, *AJ*, 114, 1002
- Zaritsky, D., Harris, J., Grebel, E. K., & Thompson, I. B. 2000, *ApJ*, 534, L53
- Zaritsky, D., Harris, J., Thompson, I. B., Grebel, E. K., & Massey, P. 2002, *AJ*, 123, 855
- Zaritsky, D., & Lin, D. N. C. 1997, *AJ*, 114, 2545
- Zaritsky, D., Sheckman, S. A., Thompson, I., Harris, J., & Lin, D. N. C. 1999, *AJ*, 117, 2268
- Zhao, H. S., 1998, *MNRAS*, 294, 139
- Zhao, H. S., 1999, *ApJ*, 527, 167
- Zhao, H. S., 2000, *ApJ*, 530, 299
- Zhao, H. S., & Evans, N. W. 2000, *ApJ*, 545, L35
- Zhao, H. S., Graff, D. S., & Guhathakurta, P. 2000, *ApJ*, 532, L37
- Zhao, H., Ibata, R. A., Lewis, G. F., & Irwin, M. J. 2003, *MNRAS*, 339, 701